International Research Journal of Innovations in Engineering and Technology (IRJIET)

ISSN (online): 2581-3048

Volume 7, Issue 1, pp 65-76, January-2023

https://doi.org/10.47001/IRJIET/2023.701011

Impacts of Wind Turbine Generator's Interfacing Technology, Capacity and the Location of Placement on IEEE 13 Node Radial Test Feeder Short Circuit Currents

[1]Kemei Peter Kirui, [2]David K Murage, [3]Peter K Kihato

[1,2,3]Department of Electrical and Electronic Engineering, Jomo Kenyatta University of Agriculture and Technology, Kenya

Authors E-mails: [1]kemei.kirui@gmail.com, [2]dkmurage25@yahoo.com, [3]pkihato@jkuat.ac.ke

***Abstract* - With the global increase in the number and the capacity of the distributed generators (DGs) penetration levels in the power systems networks', there is need for a detailed assessment of the impacts the DGs have on the power systems operations. The distribution network topology, control and protection philosophies are all designed to extract power from the transmission network and distribute it to the loads. The distribution network is not designed to have generators directly connected into it hence its power flow is unidirectional from the main utility grid to the loads. During a short circuit, the presence of DGs in a distribution network creates an increase in the short circuit current levels of the distribution network and a bi-directional power flow.**

A wind turbine generator (WTGs) is one of the most commonly utilized form of renewable energy largely integrated into the distribution networks. An important aspect of the WTGs impacts studies is to evaluate their short circuit current contribution into the distribution network under different fault conditions. The IEEE 13 node radial test feeder was modelled for the short circuit study in electrical transient analysis program (ETAP) software. The short circuit study was then performed on the radial test feeder firstly without WTGs connected and secondly with different WTG interfacing models connected at various nodes on the 13 node radial test feeder. Four models utilizing either the induction machines or the synchronous machines were simulated in ETAP for the WTG interfacing. The four models were classified as Type I, Type II, Type III and Type IV WTGs.

Placement of the four models of the WTGs, Type I, Type II, Type III and Type IV WTGs created an increase in both the three phase and the SLG short circuit fault currents levels of the test feeder. Of the four models the Type I, Type II and Type III WTGs displayed similar characteristics in the increase in both the three phase and the SLG fault currents levels hence the three models were represented as one WTG model and referenced as a doubly fed induction generator (DFIG) machine. The Type IV WTG model was the only unique machine in how it impacted on the fault currents hence it was studied alone. The two WTG models, that is the DFIG machine and the Type IV machine, were then broadly classified as the two main interfacing technologies utilized in the WTG modelling from either the induction machines or the synchronous machines. This paper presents a detailed investigation on the impacts the two WTG interfacing technologies, the DFIG and the Type IV WTG models with their capacities being varied from 1MW to 3MW have on both the three phase fault currents and the SLG fault currents occurring at selected nodes of the IEEE 13 node radial test feeder chosen for the study.

Keywords: DFIG, Type IV WTG, Three Phase Fault, SLG Fault.

I. DISTRIBUTED GENERATION INTERFACING TECHNOLOGIES

All the DGs fall into two major categories regarding their modes of interfacing with the main grid, the directly interfaced distributed generators (DIDG) and the inverter interfaced distributed generators (IIDG)[1]. DG interfacing technologies provides the necessary connection to allow a DG unit to be operated in parallel with the main utility grid. The interfacing requirements established at the point of common coupling between the main utility grid and the DG address the concerns of both the DG owners and the utility and it should satisfy the main utility requirements before the DG is connected to the main grid [2][3].

There are three basic interfacing technologies for the DGs into the electrical distribution network as described below.

International Research Journal of Innovations in Engineering and Technology (IRJIET)

ISSN (online): 2581-3048

Volume 7, Issue 1, pp 65-76, January-2023

https://doi.org/10.47001/IRJIET/2023.701011

i) Synchronous Generator

Synchronous generators are conventional electric generators which convert mechanical power into electric power. They generate both active and reactive power. Since the size and the capacity of most of the DGs is small as compared to the larger main grid network, most DGs are not sufficient to regulate the voltage of the main grid hence DGs based on the synchronous generator technology are generally operated with unity power factor and they supply only the active power [4].

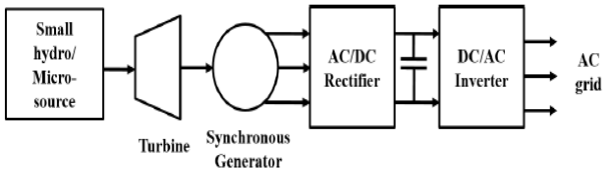

Figure 1: Block Diagram of Synchronous Generator Interfaced DG System

The output power from small hydro turbines or micro-turbines cannot be directly connected to the grid due to power quality and transient issues associated to them, hence they are interfaced using power electronic converters, where the output power is first rectified and then converted to AC using an inverter.

ii) Induction Generator

Induction generators are induction machines that convert mechanical power into electrical power when rotated at speeds greater than the synchronous speed. They are mainly used with wind turbines and some low-head hydro applications. The major advantages of the use of induction generators are that they are relatively less expensive, they require less maintenance and are robust compared to synchronous generators however, they require reactive power to operate which needs to be supplied either from the electric power system network itself or from independent sources like the capacitor banks hence they cannot be operated in the island mode. During under voltage situations, induction generators decrease the system voltage and cause serious voltage stability problems [4]. They cannot be started directly on line as they can cause transients due to inrush currents [4].

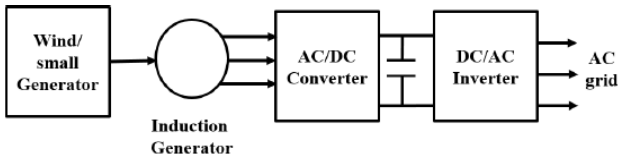

Figure 2: Block Diagram of Induction Generator Interfaced DG System

iii) Power Electronic Converter

DGs utilizing renewable energy sources like fuel cells, photovoltaic cells and battery storage generate DC power. This power is first converted to AC power of desired voltage and frequency using DC/DC power converter and fed into a DC/AC power inverter as shown in Figure 3.

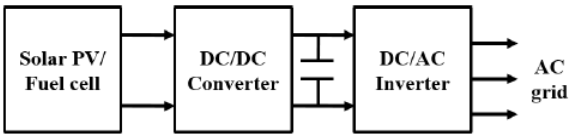

Figure 3: Block Diagram of a Power Electronics Converter Interfaced DG System

The advantage of using inverters is that they respond very quickly to the load changes and in the events of faults and this has enabled the application of islanding operation in micro-grids however, due to them having no inertia component it cannot provide energy buffer during step load changes [6].

II. WIND TURBINE GENERATOR TECHNOLOGIES

i) Type I Wind Turbine Generator

Type I WTG drives a pitch-regulated squirrel cage induction generator and is directly coupled to the grid as shown in Figure 4. Type I WTG experiences large torque swings which occur due to high wind speeds during turbulence creating a poor power factor hence compensating capacitor banks are used to couple it into the main grid [5][6].

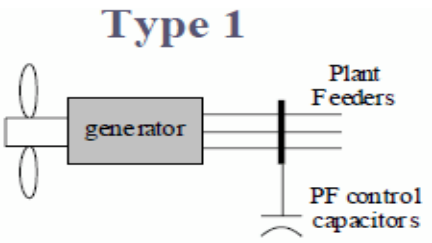

Figure 4: Type I Wind Turbine Generator

ii) Type II Wind Turbine Generator

It is an induction generator operating at variable slip. It utilizes a wound rotor induction generator whose rotor windings are brought out via slip rings and brushes and then coupled to a resistive bank as shown in Figure 5 [5]. A disadvantage of using the Type I WTG is the large torque swings that occur with turbulence in the wind speed hence by varying the resistance of the rotor windings of the Type II WTG, a more dynamic response to wind turbulence can be achieved by allowing a change in speed in the generator rotor reducing the large torque swings hence prolonging the life of the mechanical components of Type II WTG. Type II WTG

International Research Journal of Innovations in Engineering and Technology (IRJIET)
ISSN (online): 2581-3048
Volume 7, Issue 1, pp 65-76, January-2023
https://doi.org/10.47001/IRJIET/2023.701011

still requires compensating capacitor banks to achieve its operations within the required typical power factor limits[7][8].

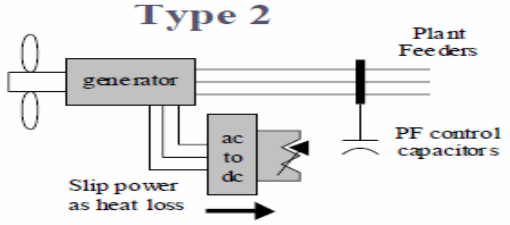

Figure 5: Type II Wind Turbine Generator

iii) Type III Wind Turbine Generator

Type III wind turbine generator is pitch-regulated wound rotor induction generator with an AC/DC/AC power converter connected between the rotor terminals and the main grid and its stator winding directly coupled to the grid hence it is commonly referred to as the doubly-fed induction generator (DFIG). Rather than its rotor windings being connected to dynamically controlled resistors, there is a power converter between the rotor windings and the grid as shown in Figure 6. The addition of the power converter between the rotor windings and the grid allows the same benefits of the Type II design without the resistive losses and the ability to provide reactive power support without external capacitor banks hence a variable speed operation that allows for a more efficient energy capture below rated wind speeds [9]. In order to protect the power converter from high short-circuit currents, protective devices such as a "crowbar" or a "chopper" circuit are used.

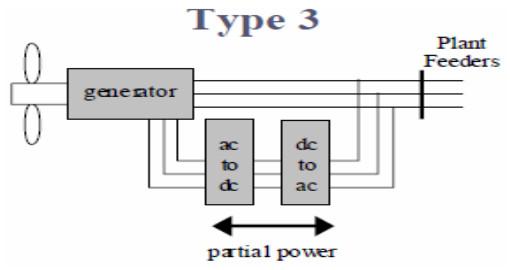

Figure 6: Type III Wind Turbine Generator

iv) Type IV Wind Turbine Generator

Type IV WTG features an AC/DC/AC power converter through which the entire power of the generator is processed. The generator may be either an induction or a synchronous type machine as shown in Figure 7. In the type IV design the wind turbine generator is decoupled from the grid through a power converter which is rated to the full output of the turbine. Since the generator is decoupled from the grid, the stator windings can operate at variable frequencies hence expanding the types of the machines that can be used with the most common being the permanent magnet synchronous machine and the squirrel cage induction machines.

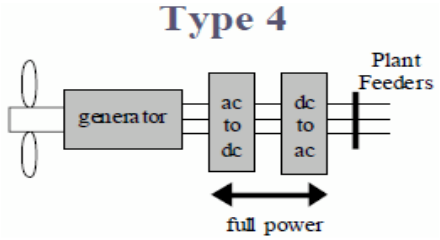

Figure 7: Type IV Wind Turbine Generator

III. WIND TURBINE GENERATORS SHORT-CIRCUIT BEHAVIORS

i) Synchronous Machine Short Circuit Model

A synchronous machine for short circuit modelling, can be represented with a Thevenin equivalent circuit where the voltage and impedance represent the worst case condition which is the highest short-circuit current contribution immediately following a fault. Figure 8 shows the Thevenin's equivalent of a synchronous machine having a sub-transient reactance equivalent of X_d''.

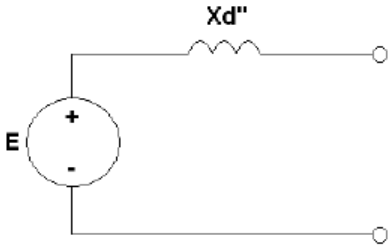

Figure 8: Synchronous Machine Short-Circuit Equivalent

Wind power plants on the other hand do not employ these types of machines for energy production. Wind power plants either employ an induction machine with a direct connection to the main electrical grid, or they decouple the induction machine from the main grid through power electronic devices.

ii) Induction Machines Short-Circuit Models

A) Type I WTG Short-Circuit Model

The major difference between an induction machine and a synchronous machine in regards to their behavior during a fault is their method/mode of excitation. For a synchronous machines the excitation is provided from an independent DC source that is unaffected by a fault occurring on the AC system. Due to this separate excitation, a synchronous machine continues to supply high transient currents

International Research Journal of Innovations in Engineering and Technology (IRJIET)
ISSN (online): 2581-3048
Volume 7, Issue 1, pp 65-76, January-2023
https://doi.org/10.47001/IRJIET/2023.701011

throughout the duration of a fault event [5]. In contrast to this, the drop in line voltage caused by a fault will cause/make the induction machine to lose its excitation hence it only supplies transient currents to the fault for one or two cycles. Most induction machines on the electric power grid are small enough such that their contribution to the fault current can be neglected, however the induction machines used to generate electrical power at the wind turbine generators power plants are large enough such that they are taken into account when determining the total fault current [9]. The equivalent machine impedance for fault calculations for a Type I WTG is the sum of the stator and rotor reactance as shown in Figure 9.

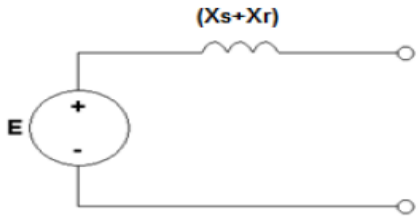

Figure 9: Sub-Transient Induction Machine Equivalent Circuit

B) Type II WTG Short-Circuit Model

The addition of the external rotor resistance to a Type II WTG acts as an impedance in the short-circuit equivalent, thus lowering the maximum available fault current of the induction machine. However, the Type II wind turbine is operated such that the external rotor resistance is applied only when necessary since the losses in the resistor bank equate to lost energy production from the generator [5]. This makes the short-circuit behavior for a Type II WTG machine similar to that of a Type I WTG machine. The same equivalent circuit for a Type I WTG machine shown in Figure 9 is also used for a Type II WTG machine.

C) Type III WTG Short-Circuit Model

The short-circuit behavior of Type III WTG is modelled differently depending on the method used in protecting its rotor power converter. Figure 10 and Figure 11 shows the two methods used to protect the power converter on the rotor circuit for the Type III WTG. The type of protective device used for the rotor converter has a significant impact on the short-circuit behavior of the Type III WTG [5].During the initial phase of a fault. The crowbar circuit diverts the short-circuit currents away from the power converter, essentially shorting out the rotor windings. The removal of the power converter during a fault makes the Type III WTG behave similar to the Type I WTG and Type II WTG design, where worst case short-circuit current is based on the internal impedance of the induction machine as shown in Figure 10. The other method of protecting the rotor converter is done with a chopper circuit [9]. With a chopper circuit, better grid support such as low voltage ride through, is achieved during a fault by keeping the rotor converter active, but still limiting the currents to protect the sensitive power electronics devices within the power converters. When this method is used the short-circuit contribution from a Type III WTG is similar to that of a Type IV WTG and the equivalent circuit is shown in Figure 11.

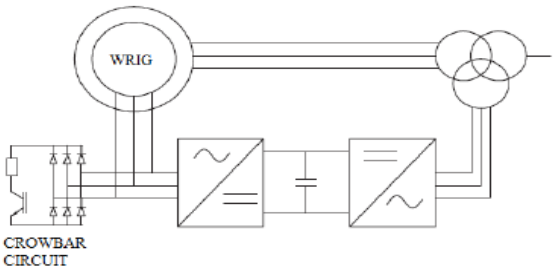

Figure 10: Type III Wind Turbines Generator Crowbar Protection of the Power Converter

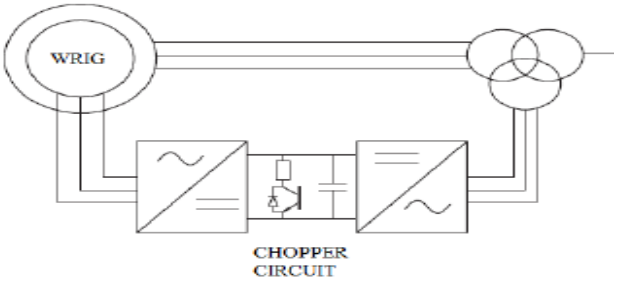

Figure 11: Type III Wind Turbines Generator Chopper Protection of the Power Converter

D) Type IV WTG Short-Circuit Model

Unlike the Type I and the Type II designs where the short-circuit behavior was dominated by the generator characteristics; it is the design of the power converter that drives the electrical behavior of the Type IV WTG. Rather than the common voltage source behind impedance short-circuit equivalent used to model most generators, the Type IV WTG is a current source designed for maximum short-circuit contribution as shown in Figure 12. The power converter in the Type III design with the chopper circuit protection is sensitive to excessive currents, so too is the converter in a Type IV WTG design [9]. So in-order to protect the power electronics devices a current limit of $1.1pu$ is designed into the power converter.

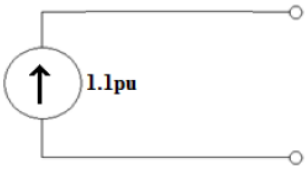

Figure 12: Type IV WTG Short-Circuit Equivalent

International Research Journal of Innovations in Engineering and Technology (IRJIET)

ISSN (online): 2581-3048

Volume 7, Issue 1, pp 65-76, January-2023

https://doi.org/10.47001/IRJIET/2023.701011

IV. IMPACTS OF WIND TURBINE GENERATORS INTERFACING TECHNOLOGY, CAPACITY AND THE LOCATION OF PLACEMENT ONIEEE 13 NODE FEEDER SHORT CIRCUIT CURRENTS

i) IEEE 13 Node Radial Test Feeder Configuration

The IEEE 13 node radial test feeder is a short, unbalanced and relatively highly loaded 4.16kV feeder. The IEEE 13 node radial test feeder has: A 5000kVA 115kV/4.16kV Delta/Star substation transformer connected at NODE650 as the main grid supply; Eight overhead distribution lines and two underground cables with variety of lengths and phasing; Unbalanced delta and star connected distributed and spot loads; Two shunt capacitor banks one having a single phase connection at NODE611 and the other a three phase connection at NODE675; and a 500kVA 4.16kV/0.48kV star/star solidly grounded in-line transformer connected between NODE633 and NODE634. Figure 10 shows the schematic layout of the IEEE 13 node radial test feeder used as the model which was simulated without showing the different connected loads or the nature and configuration of the distribution components of the feeder [10]. The short circuit currents contribution by the motoring loads was considered minimal at 1% of their Locked-Rotor Current (LRC) while the short circuit contribution by the WTGs is set at 600% of their LRC.

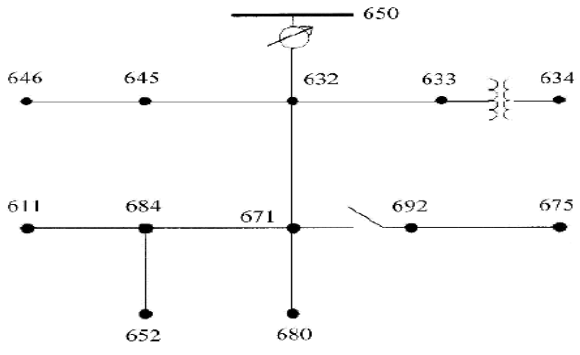

Figure 13: The IEEE 13 Node Radial Test Feeder Schematic Diagram

Four nodes were then chosen for the placement of the WTGs. The choice of the nodes was based on the distance the nodes are/were located from the main grid substation. The nodes were: NODE650 zero feet away, NODE632 2000 feet away, NODE671 4000 feet away and finally NODE680 5000 feet away from the main grid substation.

NODE652, though being the farthest node from the main grid substation at 5100 feet, had a single phase connection with an underground cable hence the reason for the choice of NODE680 for WTG placement as the farthest node at 5000 feet because it has a three phase overhead line interconnecting it with the rest of the test feeder nodes.

All the chosen nodes for WTG placement are/were three phase nodes with three phase overhead lines interconnecting them with the rest of the test feeder node.

Four nodes were again chosen to study the impacts the two WTG interfacing technologies have on the variations on the radial test feeder three phase and SLG short circuit fault currents. The four nodes chosen for the study were: NODE650 zero feet away from the main grid; NODE632 2000 feet away from the main grid; NODE671 4000 feet away from the main grid and finally NODE652 which was the farthest node at 5100 feet away from the main grid.

The two WTG interfacing technologies, the DFIG and the Type IV were interchangeably connected at nodes: NODE650, NODE632, NODE671 and NODE680 with their capacities being varied from 1MW to 3MW to analyze the impacts the increase on the DFIG and the Type IV WTG capacities have on the short circuit currents at NODE650, NODE632, NODE671 and NODE652.

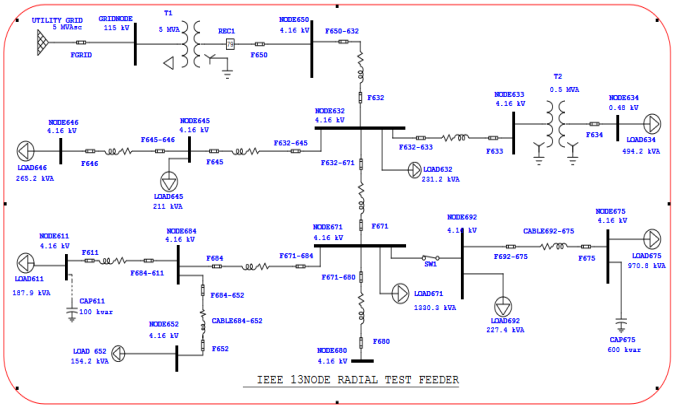

Figure 14: IEEE 13 Node Radial Test Feeder ETAP Model One-Line Diagram

ii) Impacts of Wind Turbine Generator Interfacing Technology, Capacity and the Location of Placement on NODE650 Short Circuit Currents

Table 1: Fault Currents without WTGs

NODE ID	Three Phase	SLG
NODE650	647	935
NODE632	609	810
NODE671	575	715
NODE652	558	671

Table 2: Three Phase Fault Currents in Amperes at NODE650 with 1MW and 3MW DFIG and Type IV WTG

WTG Location	DFIG		Type IV WTG	
	1MW DFIG	3MW DFIG	1MW Type IV	3MW Type IV
NODE650	1624	3582	719	1037

International Research Journal of Innovations in Engineering and Technology (IRJIET)

ISSN (online): 2581-3048

Volume 7, Issue 1, pp 65-76, January-2023

https://doi.org/10.47001/IRJIET/2023.701011

NODE632	1540	2939	723	1054
NODE671	1470	2523	727	1067
NODE680	1439	2367	729	1071

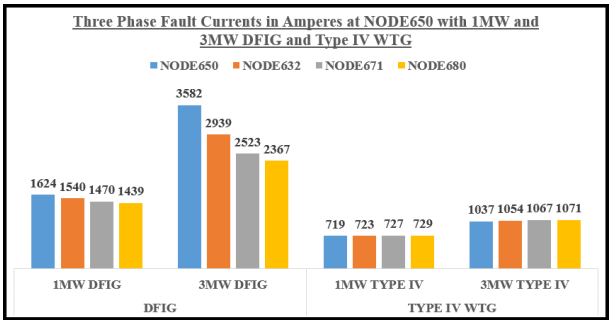

Chart 1: Three Phase Fault Currents in Amperes at NODE650 with 1MW and 3MW DFIG and Type IV WTG

When the radial test feeder was short circuited without WTG connected into it, the three phase short circuit fault currents at NODE650 was 647A as seen from Table 1. This value of 647A would increase in magnitude to 1624A when the radial test feeder was again short circuited but now with a 1MW DFIG connected at NODE650. As the 1MW DFIGs were placed farther away from the faulted NODE650, the three phase fault currents at the faulted NODE650 reduced from 1624A to: 1540A when the 1MW DFIG was connected at NODE632 2000 feet away from the faulted node; 1470A when the 1MW DFIG was connected at NODE671 4000 feet away from the faulted node; and finally to 1439A when the 1MW DFIG was connected at NODE680 5000 feet away from the faulted node as seen from Table 2 and chart 1.

The three phase short circuit fault currents at the faulted NODE650 would again increase: From 1624A to 3582A when the capacity of the DFIG connected at NODE650 was increased from 1MW to 3MW; From 1540A to 2939A when the capacity of the DFIG connected at NODE632 was increased from 1MW to 3MW; From 1470A to 2523A when the capacity of the DFIG connected at NODE671 was increased from 1MW to 3MW; and finally from 1439A to 2367A when the capacity of the DFIG connected at NODE680 was increased from 1MW to 3MW as seen from Table 2 and chart 1.

For Type IV WTGs, the three phase short circuit fault currents at the faulted NODE650 was 719A when a 1MW Type IV WTG was connected at NODE650. This value of 719A would gradually increase to: 723A when the 1MW Type IV WTG was connected at NODE632; 727A when the 1MW Type IV WTG was connected at NODE671; and finally 729A when the 1MW Type IV WTG was connected at NODE680 as can be seen from Table 2 and chart 1.

When a 3MW Type IV WTGs was connected at NODE650, the three phase short circuit fault currents at the faulted NODE650 increased to 1037A up from 719A when a 1MW Type IV WTG was connected at NODE650. The value of the three phase short circuit fault currents at NODE650 would gradually increase from 1037A to: 1054A when the 3MW Type IV WTG was connected at NODE632; 1067A when the 3MW Type IV WTG was connected at NODE671; and finally 1071A when the 3MW Type IV WTG was connected at NODE680 as can be seen from Table 2 and chart 1.

Table 3: Single-Line-to-Ground Fault Currents in Amperes at NODE650 with 1MW and 3MW DFIG and Type IV WTG

WTG Location	DFIG		Type IV WTG	
	1MW DFIG	3MW DFIG	1MW Type IV	3MW Type IV
NODE650	2298	4798	1038	1487
NODE632	2178	3936	1044	1510
NODE671	2078	3404	1049	1525
NODE680	2035	3205	1052	1531

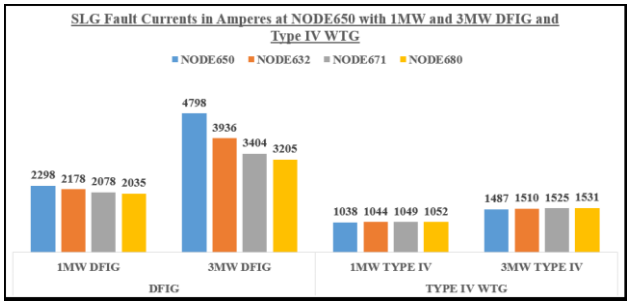

Chart 2: Single-Line-to-Ground Fault Currents in Amperes at NODE650 with 1MW and 3MW DFIG and Type IV WTG

Without WTGs connected into the test feeder, the SLG short circuit fault currents at NODE650 was 935A as seen from Table 1. This value of 935A would increase in magnitude to 2298A when the radial test feeder was again short circuited but now with a 1MW DFIG connected at NODE650. As the 1MW DFIGs were placed farther away from the faulted NODE650, the SLG fault currents reduced from 2298A to: 2178A when the 1MW DFIG was connected at NODE632; 2078A when the 1MW DFIG was connected at NODE671; and finally to 2035A when the 1MW DFIG was connected at NODE680 as seen from Table 3 and chart 2.

The SLG short circuit fault currents at the faulted NODE650 would again increase: From 2298A to 4798A when the capacity of the DFIG connected at NODE650 was increased from 1MW to 3MW; From 2178A to 3936A when the capacity of the DFIG connected at NODE632 was increased from 1MW to 3MW; From 2078A to 3404A when the capacity of the DFIG connected at NODE671 was

International Research Journal of Innovations in Engineering and Technology (IRJIET)

ISSN (online): 2581-3048

Volume 7, Issue 1, pp 65-76, January-2023

https://doi.org/10.47001/IRJIET/2023.701011

increased from 1MW to 3MW and finally it increased from 2035A to 3205A when the capacity of the DFIG connected at NODE680 was increased from 1MW to 3MW as seen from Table 3 and chart 2.

For Type IV WTGs, the SLG short circuit fault currents at the faulted NODE650 were 1038A when a 1MW Type IV WTG was connected at NODE650. This value of 1038A would gradually increase to: 1044A when the 1MW Type IV WTG was connected at NODE632; 1049A when the 1MW Type IV WTG was connected at NODE671; and finally 1052A when the 1MW Type IV WTG was connected at NODE680 as seen from Table 3 and chart 2.

When a 3MW Type IV WTGs was connected at NODE650, the SLG short circuit fault currents at the faulted NODE650 increased to 1487A up from 1038A when a 1MW Type IV WTG was connected at NODE650. The value of the SLG short circuit fault currents at NODE650 would again gradually increase from 1487A to: 1510A when a 3MW Type IV WTG was connected at NODE632; 1525A when a 3MW Type IV WTG was connected at NODE671; and finally 1531A when a 3MW Type IV WTG was connected at NODE680 as can be seen from Table 3 and chart 2.

iii) Impacts of Wind Turbine Generator Interfacing Technology, Capacity and the Location of Placement on NODE632 Short Circuit Currents

Table 4: Three Phase Fault Currents in Amperes at NODE632 with 1MW and 3MW DFIG and Type IV WTG

WTG Location	DFIG		Type IV WTG	
	1MW DFIG	3MW DFIG	1MW Type IV	3MW Type IV
NODE632	1586	3544	686	1015
NODE671	1503	2901	690	1031
NODE650	1406	2668	673	958
NODE680	1466	2674	692	1037

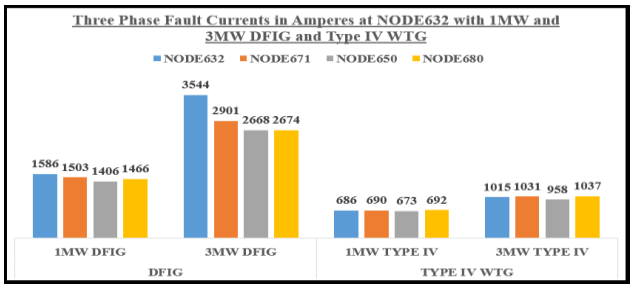

Chart 3: Three Phase Fault Currents in Amperes at NODE632 with 1MW and 3MW DFIG and Type IV WTG

When the radial test feeder was short circuited without WTG connected into it, the three phase short circuit fault currents at NODE632 was 609A as seen from Table 1. This value of 609A would increase in magnitude to 1586A when the radial test feeder was again short circuited but now with a 1MW DFIG connected at NODE632. As the 1MW DFIGs were placed farther away from the faulted NODE632, the three phase fault currents at the faulted NODE632 reduced from 1586A to: 1503A when the 1MW DFIG was connected at NODE671 2000 feet away from the faulted node; 1466A when the 1MW DFIG was connected at NODE680 3000 feet away from the faulted node; and finally to 1406A when the 1MW DFIG was connected at NODE650 2000 feet away from the faulted node as seen from Table 4 and chart 3.

The three phase short circuit fault currents at the faulted NODE632 would again increase: From 1586A to 3544A when the capacity of the DFIG connected at NODE632 was increased from 1MW to 3MW; From 1503A to 2901A when the capacity of the DFIG connected at NODE671 was increased from 1MW to 3MW; From 1466A to 2674A when the capacity of the DFIG connected at NODE680 was increased from 1MW to 3MW; and finally from 1406A to 2668A when the capacity of the DFIG connected at NODE650 was increased from 1MW to 3MW as seen from Table 4 and chart 3.

For Type IV WTGs, the three phase short circuit fault currents at the faulted NODE632 was 673A when a 1MW Type IV WTG was connected at NODE650. This value of 673A would gradually increase to: 686A when the 1MW Type IV WTG was connected at NODE632; 690A when the 1MW Type IV WTG was connected at NODE671; and finally 692A when the 1MW Type IV WTG was connected at NODE680 as can be seen from Table 4 and chart 3.

When a 3MW Type IV WTGs was connected at NODE650, the three phase short circuit fault currents at the faulted NODE632 increased to 958A up from 673A when a 1MW Type IV WTG was connected at NODE650. The value of the three phase short circuit fault currents at NODE632 would gradually increase from 958A to: 1015A when the 3MW Type IV WTG was connected at NODE632; 1031A when the 3MW Type IV WTG was connected at NODE671; and finally 1037A when the 3MW Type IV WTG was connected at NODE680 as can be seen from Table 4 and chart 3.

Table 5: Single-Line-to-Ground Fault Currents in Amperes at NODE632 with 1MW and 3MW DFIG and Type IV WTG

WTG Location	DFIG		Type IV WTG	
	1MW DFIG	3MW DFIG	1MW Type IV	3MW Type IV
NODE632	1973	4129	904	1293
NODE671	1858	3255	909	1316
NODE650	1669	2683	887	1225

International Research Journal of Innovations in Engineering and Technology (IRJIET)

ISSN (online): 2581-3048

Volume 7, Issue 1, pp 65-76, January-2023

https://doi.org/10.47001/IRJIET/2023.701011

NODE680	1810	2992	912	1325

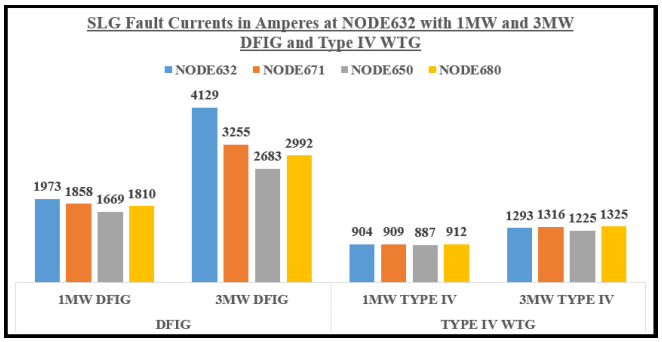

Chart 4: Single-Line-to-Ground Fault Currents in Amperes at NODE632 with 1MW and 3MW DFIG and Type IV WTG

Without WTGs connected into the test feeder, the SLG short circuit fault currents at NODE632 was 810A as seen from Table 1. This value of 810A would increase in magnitude to 1973A when the radial test feeder was again short circuited but now with a 1MW DFIG connected at NODE632. As the 1MW DFIGs were placed farther away from the faulted NODE632, the SLG fault currents reduced from 1973A to: 1858A when the 1MW DFIG was connected at NODE671; 1810A when the 1MW DFIG was connected at NODE680; and finally to 1669A when the 1MW DFIG was connected at NODE650 as seen from Table 5 and chart 4.

The SLG short circuit fault currents at the faulted NODE632 would again increase: From 1973A to 4129A when the capacity of the DFIG connected at NODE632 was increased from 1MW to 3MW; From 1858A to 3255A when the capacity of the DFIG connected at NODE671 was increased from 1MW to 3MW; From 1810A to 2992A when the capacity of the DFIG connected at NODE680 was increased from 1MW to 3MW and finally it increased from 1669A to 2683A when the capacity of the DFIG connected at NODE650 was increased from 1MW to 3MW as seen from Table 5 and chart 4.

For Type IV WTGs, the SLG short circuit fault currents at the faulted NODE632 were 887A when a 1MW Type IV WTG was connected at NODE650. This value of 887A would gradually increase to: 904A when the 1MW Type IV WTG was connected at NODE632; 909A when the 1MW Type IV WTG was connected at NODE671; and finally 912A when the 1MW Type IV WTG was connected at NODE680 as seen from Table 5 and chart 4.

When a 3MW Type IV WTGs was connected at NODE650, the SLG short circuit fault currents at the faulted NODE632 increased to 1225A up from 887A when a 1MW Type IV WTG was connected at NODE650. This value of the SLG short circuit fault currents at NODE632 would again gradually increase from 1225A to: 1293A when the 3MW Type IV WTG was connected at NODE632; 1316A when the 3MW Type IV WTG was connected at NODE671; and finally 1325A when a 3MW Type IV WTG was connected at NODE680 as can be seen from Table 5 and chart 4.

iv) Impacts of Wind Turbine Generator Interfacing Technology, Capacity and the Location of Placement on NODE671 Short Circuit Currents

Table 6: Three Phase Fault Currents in Amperes at NODE671 with 1MW and 3MW DFIG and Type IV WTG

WTG Location	DFIG		Type IV WTG	
	1MW DFIG	3MW DFIG	1MW Type IV	3MW Type IV
NODE671	1552	3510	656	995
NODE680	1509	3151	658	1003
NODE632	1377	2647	644	940
N0DE650	1239	2122	633	888

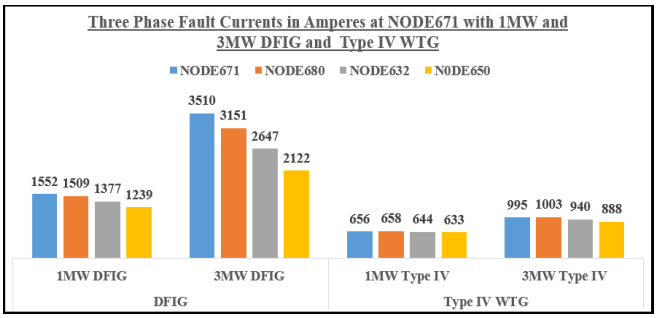

Chart 5: Three Phase Fault Currents in Amperes at NODE671 with 1MW and 3MW DFIG and Type IV WTG

When the radial test feeder was short circuited without WTG connected into it, the three phase short circuit fault currents at NODE671 was 575A as seen from Table 1. This value of 575A would increase in magnitude to 1552A when the radial test feeder was again short circuited but now with a 1MW DFIG connected at NODE671. As the 1MW DFIGs were placed farther away from the faulted NODE671, the three phase fault currents at the faulted NODE671 reduced from 1552A to: 1509A when the 1MW DFIG was connected at NODE680 1000 feet away from the faulted node; 1377A when the 1MW DFIG was connected at NODE632 2000 feet away from the faulted node; and finally to 1239A when the 1MW DFIG was connected at NODE650 4000 feet away from the faulted node as seen from Table 6 and chart 5.

The three phase short circuit fault currents at the faulted NODE671 would again increase: From 1552A to 3510A when the capacity of the DFIG connected at NODE671 was increased from 1MW to 3MW; From 1509A to 3151A when the capacity of the DFIG connected at NODE680 was increased from 1MW to 3MW; From 1377A to 2647A when

International Research Journal of Innovations in Engineering and Technology (IRJIET)
ISSN (online): 2581-3048
Volume 7, Issue 1, pp 65-76, January-2023
https://doi.org/10.47001/IRJIET/2023.701011

the capacity of the DFIG connected at NODE632 was increased from 1MW to 3MW; and finally from 1239A to 2122A when the capacity of the DFIG connected at NODE650 was increased from 1MW to 3MW as seen from Table 6 and chart 5.

For Type IV WTGs, the three phase short circuit fault currents at the faulted NODE671 was 633A when a 1MW Type IV WTG was connected at NODE650. This value of 633A would gradually increase to: 644A when the 1MW Type IV WTG was connected at NODE632; 656A when the 1MW Type IV WTG was connected at NODE671; and finally 658A when the 1MW Type IV WTG was connected at NODE680 as can be seen from Table 6 and chart 5.

When a 3MW Type IV WTGs was connected at NODE650, the three phase short circuit fault currents at the faulted NODE671 increased to 888A up from 633A when a 1MW Type IV WTG was connected at NODE650. The value of the three phase short circuit fault currents at NODE671 would gradually increase from 888A to: 940A when the 3MW Type IV WTG was connected at NODE632; 995A when the 3MW Type IV WTG was connected at NODE671; and finally 1003A when the 3MW Type IV WTG was connected at NODE680 as can be seen from Table 6 and chart 5.

Table 7: Single-Line-to-Ground Fault Currents in Amperes at NODE671 with 1MW and 3MW DFIG and Type IV WTG

WTG Location	DFIG		Type IV WTG	
	1MW DFIG	3MW DFIG	1MW Type IV	3MW Type IV
NODE671	1799	3889	804	1166
NODE680	1734	3335	807	1180
NODE632	1489	2459	787	1091
N0DE650	1308	1857	774	1034

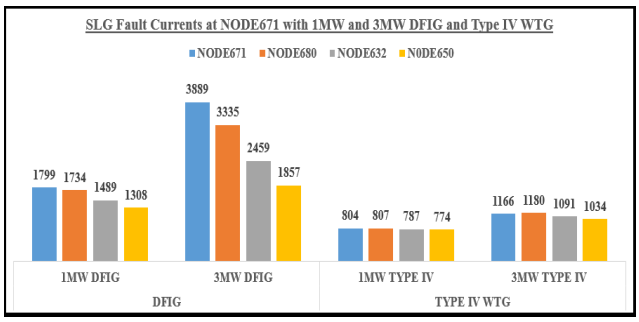

Chart 6: Single-Line-to-Ground Fault Currents in Amperes at NODE671 with 1MW and 3MW DFIG and Type IV WTG

Without WTGs connected into the test feeder, the SLG short circuit fault currents at NODE671 was 715A as seen from Table 1. This value of 715A would increase in magnitude to 1799A when the radial test feeder was again short circuited but now with a 1MW DFIG connected at NODE671. As the 1MW DFIGs were placed farther away from the faulted NODE671, the SLG fault currents reduced from 1799A to: 1734A when the 1MW DFIG was connected at NODE680; 1489A when the 1MW DFIG was connected at NODE632; and finally to 1308A when the 1MW DFIG was connected at NODE650 as seen from Table 7 and chart 6.

The SLG short circuit fault currents at the faulted NODE671 would again increase: From 1799A to 3889A when the capacity of the DFIG connected at NODE671 was increased from 1MW to 3MW; From 1734A to 3335A when the capacity of the DFIG connected at NODE680 was increased from 1MW to 3MW; From 1489A to 2459A when the capacity of the DFIG connected at NODE632 was increased from 1MW to 3MW and finally it increased from 1308A to 1857A when the capacity of the DFIG connected at NODE650 was increased from 1MW to 3MW as seen from Table 7 and chart 6.

For Type IV WTGs, the SLG short circuit fault currents at the faulted NODE671 were 774A when a 1MW Type IV WTG was connected at NODE650. This value of 774A would gradually increase to: 787A when the 1MW Type IV WTG was connected at NODE632; 804A when the 1MW Type IV WTG was connected at NODE671; and finally 807A when the 1MW Type IV WTG was connected at NODE680 as seen from Table 7 and chart 6.

When the capacity of the Type IV WTGs connected at NODE650 was increased from 1MW to 3MW, the SLG short circuit fault currents at the faulted NODE671 increased to 1034A up from 774A. This value of the SLG short circuit fault currents at NODE671 would again gradually increase from 1034A to: 1091A when the 3MW Type IV WTG was connected at NODE632; 1166A when the 3MW Type IV WTG was connected at NODE671; and finally 1180A when the 3MW Type IV WTG was connected at NODE680 as can be seen from Table 7 and chart 6.

v) Impacts of Wind Turbine Generator Interfacing Technology, Capacity and the Location of Placement on NODE652 Short Circuit Currents

Table 8: Three Phase Fault Currents in Amperes at NODE652 with 1MW and 3MW DFIG and Type IV WTG

WTG Location	DFIG		Type IV WTG	
	1MW DFIG	3MW DFIG	1MW Type IV	3MW Type IV
NODE671	1434	2925	623	907
NODE680	1396	2665	625	914
NODE632	1281	2290	613	862
NODE650	1159	1883	603	819

International Research Journal of Innovations in Engineering and Technology (IRJIET)

ISSN (online): 2581-3048

Volume 7, Issue 1, pp 65-76, January-2023

https://doi.org/10.47001/IRJIET/2023.701011

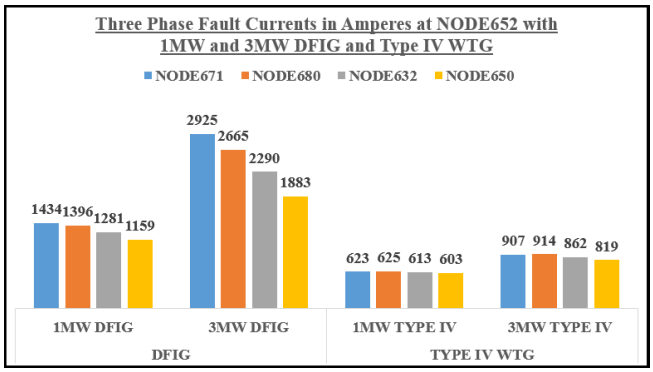

Chart 7: Three Phase Fault Currents in Amperes at NODE652 with 1MW and 3MW DFIG and Type IV WTG

When the radial test feeder was short circuited without WTG connected into it, the three phase short circuit fault currents at NODE652 was 558A as seen from Table 1. This value of 558A would increase in magnitude to 1434A when the radial test feeder was again short circuited but now with a 1MW DFIG connected at NODE671. As the 1MW DFIGs were placed farther away from the faulted NODE652, the three phase fault currents at the faulted NODE652 reduced from 1434A to: 1396A when the 1MW DFIG was connected at NODE680 2100 feet away from the faulted node; 1281A when the 1MW DFIG was connected at NODE632 3100 feet away from the faulted node; and finally to 1159A when the 1MW DFIG was connected at NODE650 5100 feet away from the faulted node as seen from Table 8 and chart 7.

The three phase short circuit fault currents at the faulted NODE652 would again increase: From 1434A to 2925A when the capacity of the DFIG connected at NODE671 was increased from 1MW to 3MW; From 1396A to 2665A when the capacity of the DFIG connected at NODE680 was increased from 1MW to 3MW; From 1281A to 2290A when the capacity of the DFIG connected at NODE632 was increased from 1MW to 3MW; and finally from 1159A to 1883A when the capacity of the DFIG connected at NODE650 was increased from 1MW to 3MW as seen from Table 8 and chart 7.

For Type IV WTGs, the three phase short circuit fault currents at the faulted NODE652 was 603A when a 1MW Type IV WTG was connected at NODE650. This value of 603A would gradually increase to: 613A when the 1MW Type IV WTG was connected at NODE632; 623A when the 1MW Type IV WTG was connected at NODE671; and finally 625A when the 1MW Type IV WTG was connected at NODE680 as can be seen from Table 8 and chart 7.

When the capacity of the Type IV WTG connected at NODE650 was increased from 1MW to 3MW, the three phase short circuit fault currents at the faulted NODE652 increased to 819A up from 603A. The value of the three phase short circuit fault currents would again gradually increase from 819A to: 862A when the 3MW Type IV WTG was connected at NODE632; 907A when the 3MW Type IV WTG was connected at NODE671; and finally 914A when the 3MW Type IV WTG was connected at NODE680 as can be seen from Table 8 and chart 7.

Table 9: Single-Line-to-Ground Fault Currents in Amperes at NODE652 with 1MW and 3MW DFIG and Type IV WTG

WTG Location	DFIG		Type IV WTG	
	1MW DFIG	3MW DFIG	1MW Type IV	3MW Type IV
NODE671	1545	2795	729	988
NODE680	1494	2488	732	1000
NODE632	1306	1965	718	939
NODE650	1162	1559	708	901

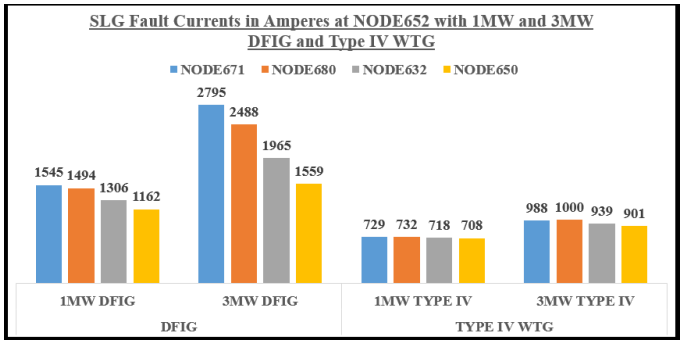

Chart 8: Single-Line-to-Ground Fault Currents in Amperes at NODE652 with 1MW and 3MW DFIG and Type IV WTG

When the radial test feeder was short circuited without WTG connected into it, the SLG short circuit fault currents at NODE652 was 671A as seen from Table 1. This value of 671A would increase in magnitude to 1545A when the radial test feeder was again short circuited but now with a 1MW DFIG connected at NODE671. As the 1MW DFIGs were placed farther away from the faulted NODE652, the SLG fault currents at the faulted NODE652 reduced from 1545A to: 1494A when the 1MW DFIG was connected at NODE680; 1306A when the 1MW DFIG was connected at NODE632; and finally to 1162A when the 1MW DFIG was connected at NODE650 as seen from Table 9 and chart 8.

The SLG short circuit fault currents at the faulted NODE652 would again increase: From 1545A to 2795A when the capacity of the DFIG connected at NODE671 was increased from 1MW to 3MW; From 1494A to 2488A when the capacity of the DFIG connected at NODE680 was increased from 1MW to 3MW; From 1306A to 1965A when the capacity of the DFIG connected at NODE632 was increased from 1MW to 3MW; and finally from 1162A to 1559A when the capacity of the DFIG connected at NODE650

ISSN (online): 2581-3048
Volume 7, Issue 1, pp 65-76, January-2023
https://doi.org/10.47001/IRJIET/2023.701011

was increased from 1MW to 3MW as seen from Table 9 and chart 8.

For Type IV WTGs, the SLG short circuit fault currents at the faulted NODE652 were 708A when a 1MW Type IV WTG was connected at NODE650. This value of 708A would gradually increase to: 718A when the 1MW Type IV WTG was connected at NODE632; 729A when the 1MW Type IV WTG was connected at NODE671; and finally 732A when the 1MW Type IV WTG was connected at NODE680 as can be seen from Table 9 and chart 8.

When the capacity of the Type IV WTG connected at NODE650 was increased from 1MW to 3MW, the SLG short circuit fault currents at the faulted NODE652 increased to 901A up from 708A. The value of the three phase short circuit fault currents would again gradually increase from 901A to: 939A when the 3MW Type IV WTG was connected at NODE632; 988A when the 3MW Type IV WTG was connected at NODE671; and finally 1000A when the 3MW Type IV WTG was connected at NODE680 as can be seen from Table 9 and chart 8.

V. CONCLUSION

WTG connection into the radial test feeder caused an increase in the short circuit current capacity of the test feeder. There was an increase in both the three phase and the SLG short circuit fault currents levels on the four nodes chosen for study that is NODE650, NODE632, NODE671 and NODE652.

The DFIG injected the highest short circuit currents into both the three phase and SLG fault occurring in the test feeder as compared to the contribution by the Type IV WTG. For both the DFIG and the Type IV WTG, an increase on the generator capacity from 1MW to 3MW further caused an increase in the three phase fault currents and the SLG fault currents. 3MW DFIG injected the highest magnitudes of both the three phase and SLG fault currents occurring in the test feeder.

The highest levels of three phase fault currents for Type IV WTG machines were experienced for Type IV WTG machines placed/connected at NODE680. The magnitudes of the three phase fault currents progressively reduced as the Type IV WTG machines were connected at NODE671, NODE632 and finally the three phase faults currents were the lowest when Type IV WTG machines were connected at NODE650.

The highest levels of the SLG fault currents for Type IV WTG machines were experienced for Type IV WTG machines placed/connected at NODE680. The magnitudes of the SLG fault currents progressively reduced as the Type IV WTG machines were connected at NODE671, NODE632 and finally the SLG faults currents were the lowest when Type IV WTG machines were connected at NODE650.

For the DFIG machines, the magnitudes of both the three phase and the SLG short circuit fault currents reduced in magnitudes as the faulted nodes are located farther away from the main grid substation NODE650.

It was therefore concluded that the point of location/distance/position for placement of WTGs impacted a lot on the magnitudes of the network short circuit fault current levels with the DFIG machines placed far away from the faulted nodes injecting the least amount into a short circuit as compared to the magnitudes of the fault currents injected by DFIGs placed closer/nearer to the faulted nodes.

REFERENCES

[1] Seema Jadhar, Ruchi Harchandani*'' Grid Interfacing Technologies for Distributed Generation and Power Quality Issues-A Review''* International Journal of Innovative and Emerging Research in Engineering Volume 2, Issue 3, 2015.

[2] Juan A. Martinez and Jacinto Martin-Arnedo "*Impact of Distributed Generation on Distribution Protection and Power Quality"* Power & energy society general meeting 26th-30th July 2009.

[3] Martin Geidl "*Protection of Power Systems with Distributed Generation: State of the Art*" Power Systems Laboratory Swiss Federal Institute of Technology (ETH) Zurich 20th July 2005.

[4] Pooria Mohammadi, Hassan El-Kishyky, Mamdouh A Akher and Mazen A Salam "*The Impacts of Distributed Generation on Fault Detection and Voltage Profile in Power Distribution Networks" IEEE Conference on* Power Modulator and High Voltage (IPMHVC) 1st - 5th June 2014.

[5] *"WECC Wind Power Plant Dynamic Modelling Guide*" Western Electricity Coordinating Council Modelling and Validation Work Group. Technical Report. April 2014.

[6] Edward Muljadi and Abraham Ellis. "*WECC Wind Generator Development"*. National Renewable Energy Laboratory. Technical Report. March 2010.

[7] Kirui K, Murage K, and Kihato K, "*Impacts of Placement of Wind Turbine Generators with Different Interfacing Technologies on Radial Distribution Feeder Short Circuit Currents.* Proceedings of sustainable research and innovation conference. JKUAT, *ISSN: 2079-6226*, Pg 206-212, Published on April 29, 2022

ISSN (online): 2581-3048
Volume 7, Issue 1, pp 65-76, January-2023
https://doi.org/10.47001/IRJIET/2023.701011

[8] J.A. Pecas Lopes, N. Hatziargyriou, J. Mutale, P.Djapic, N. Jenkins. *"Integrating Distributed Generation into Electric Power Systems: A review of drivers, challenges and opportunities*" Science Direct. Electrical Power Systems Research 77(2007) 1189-1203.ELSEVIER.

[9] "*IEEE Standard for Interconnecting Distributed Resources with Electric Power Systems*" Standards Coordinating Committee 21, 28 July, 2003.

[10] W.H.Kersting, *"Radial Distribution Test Feeders"* IEEE Power engineering society. Distribution systems analysis subcommittee report. 2000.

AUTHOR'S BIOGRAPHY

Mr. Kemei Peter Kirui is a Kenyan born at Kiptere Location, Kericho County on 14th May 1983. He trained as an Electrical Engineer and graduated with a Bachelor's degree in Electrical and Communication Engineering from Moi University, Kenya and an Msc in Electrical Engineering from JKUAT Kenya. He also trained in Technology Education and graduated with a PGDE in Technology Education from Moi University, Kenya. Mr. Kemei is a registered graduate engineer by the Kenya Engineers Registration Board (ERB) and a trained Energy Auditor by Kenya Association of Manufacturers (KAM). His areas of interest in research are: Power Systems Protection; Power Systems Distribution Network Planning; and Renewable Energy Technologies.

Citation of this Article:

Kemei Peter Kirui, David K Murage, Peter K Kihato, "Impacts of Wind Turbine Generator's Interfacing Technology, Capacity and the Location of Placement on IEEE 13 Node Radial Test Feeder Short Circuit Currents" Published in *International Research Journal of Innovations in Engineering and Technology - IRJIET*, Volume 7, Issue 1, pp 65-76, January 2023. Article DOI https://doi.org/10.47001/IRJIET/2023.701011

****

